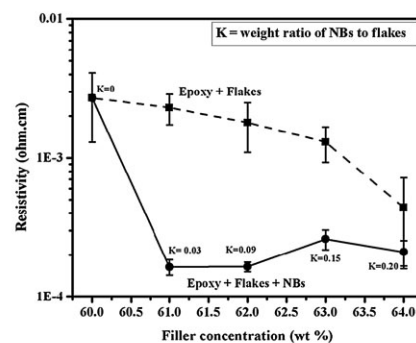
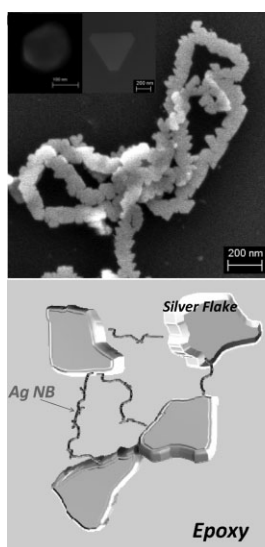


Electrical Conductive Adhesives Enhanced with High-Aspect-Ratio Silver Nanobelts

Behnam Meschi Amoli, Ehsan Marzbanrad, Anming Hu, Y. Norman Zhou, Boxin Zhao*

The utilization of high-aspect-ratio silver nanobelts (NBs) is reported with the typical silver micro flakes to develop advanced electrical conductive adhesive (ECA) composite materials. Ag NBs (10–40 nm thick, 100–400 nm wide and 1–10 μm long) were synthesized by chemical reduction of silver nitride. The incorporation of a small amount of the Ag NBs (NBs to flakes weight-ratio $K = 0.03$) into a conventional ECA with 60 wt% Ag micro flakes results in an electrical conductivity enhancement by 1300%. It is also found that adding a 2 wt% ($K = 0.03$) of the NBs into a conventional ECA with 80 wt% Ag flakes reduced the bulk resistivity to $3 \times 10^{-5} \Omega \cdot \text{cm}$ for the hybrid ECAs, which is comparable to that of a typical eutectic solder, showing great potential as an alternative electrical interconnect materials.



1. Introduction

Electrical conductive adhesives (ECAs), as one of the most promising alternatives for lead-based solders, have attracted intensive attentions in the wide range of

applications during the last two decades.^[1,2] In general, ECAs offer numerous advantages (e.g., less environmental impact, milder operating temperature, fewer processing steps, and finer pitch capability) over traditional lead-based solders.^[3–5] However, the current available ECAs still cannot completely replace the traditional solders because of their relatively low electrical conductivity. Replacement of lead-based solders with ECAs requires advanced materials with desired electrical conductivity and mechanical strength, resembling those of the metallic solders.^[6–8] In conventional ECAs, which mainly consist of silver flakes and epoxy resin, improvement of one of these fundamental properties (electrical vs. mechanical) essentially leads to sacrifice of the other. In other words, electrical conductivity enhancement of conventional ECAs requires more filler to be added into the epoxy matrix; but the addition of a large amount of filler is detrimental to the mechanical strength of the final composite due to the reduced volume fraction of the polymer matrix. In addition, it should be noted that

B. M. Amoli, B. Zhao

Department of Chemical Engineering, University of Waterloo,
200 University Avenue West, Waterloo, ON N2L 3G1, Canada
E-mail: zhaob@uwaterloo.ca

E. Marzbanrad, A. Hu, Y. N. Zhou

Department of Mechanical and Mechatronics Engineering,
University of Waterloo, 200 University Avenue West, Waterloo,
ON N2L 3G1, Canada

B. M. Amoli, Y. N. Zhou, B. Zhao

Waterloo Institute for Nanotechnology, University of Waterloo,
200 University Avenue West, Waterloo, ON N2L 3G1, Canada

E. Marzbanrad, A. Hu, Y. N. Zhou

Centre for Advanced Materials Joining, University of Waterloo,
200 University Avenue West, Waterloo, ON N2L 3G1, Canada

adding more conductive filler to epoxy after a specific concentration (i.e., percolation threshold) would not significantly improve the electrical conductivity. To address these concerns, the research works have been stepped up to implement hybrid filler systems (i.e., synergetic combination of nano-sized conductive materials and silver micro flakes) to develop cost-effective ECAs with desired properties.^[9–11]

The incorporation of spherical silver nanoparticles (NPs) to the system of epoxy and silver microflakes has been widely investigated.^[11–13] Generally, it has been believed that adding silver NPs below the “percolation” concentration improves the electrical conductivity of the ECAs while beyond that it may reduce the electrical conductivity. This negative effect has been found as a result of the increased number of contact points among the micro and nano-sized fillers;^[14] a large number of contact points increases the contact resistance and reduce the efficiency of the electrical network to transfer electrons. To overcome this drawback of adding NPs, sintering between NPs during the curing of ECAs is suggested to decrease the number of contact points and subsequently to increase the electrical conductivity.^[11,13] It has also been reported that adding very small silver NPs (less than 10 nm) can improve the electrical conductivity of the ECAs at a relatively lower curing temperature ($\approx 150^\circ\text{C}$) because such small NPs can readily fill the gaps between the micro flakes while they can also be partially sintered.^[9,10] Despite the success of spherical NPs in the enhancement of electrical conductivity of ECAs, a large amount of silver NPs, as needed to form a percolated network, can negatively influence the mechanical strength and processability of the final ECAs.

In recent years, high-aspect-ratio nanofillers have been proposed as alternative materials for spherical NPs to overcome the concern of excessive contact points between NPs and to reduce the amount of conductive fillers.^[6,7,8,15–23] High-aspect-ratio nanomaterials can establish more stable and effective electrical network at lower filler contents with less number of contact points. Moreover, they can provide better electrical conductivity without sacrificing the integrity and adhesive strength of the polymeric matrix.^[15] For instance, Wu et al. reported a significant electrical conductivity improvement for the ECAs filled with 56 wt.-% silver nanowires (NWs) compared to that of the ECAs filled with micron-sized and/or nano-sized spherical silver particles with similar filler concentration.^[15] The same results were reported by Tao et al.^[8,18] and Chen et al.^[21] However, most of the studies performed in this field have involved the direct addition of silver NWs into epoxy resin without silver flakes; this situation requires a large amount of silver NWs to achieve the desired conductivities.^[15,18,21] There are not many research activities on the development of hybrid filler systems by using high aspect-ratio silver nanomaterials as auxiliary

fillers in the formulation of the conventional ECAs. To the best of our knowledge, only Zhang et al.^[24] reported the use of silver NWs along with the silver flakes (weight ratio of 2:3) to develop a hybrid fillers system and found a significant improvement in electrical conductivity of the fabricated ECA. This study suggested a synergetic effect of high aspect-ratio silver NWs and silver flakes on the electrical conductivity improvement of the hybrid ECAs.

In this paper, we report the incorporation of a new class of high aspect-ratio nanofillers [i.e., silver nanobelts (NBs)] in a conventional ECA to develop a hybrid ECA composite. The silver NBs were synthesized through a high-yield chemical reduction method which was based on the self-assembly and room-temperature joining of the hexagonal and triangular silver NPs as structural blocks of the NBs. Compared to the previously used silver NWs which are synthesized at high temperatures and long reaction times, the fabrication of the NBs is fast and occurs at room temperature.^[25] Besides, the Ag NBs have a low “weight to length” ratio, which can reduce the total mass of the filler in the composite. Moreover, the high aspect-ratio NBs are able to form a percolated network at low concentrations. Our results revealed a significant improvement in the electrical conductivity of the hybrid ECA composite in comparison to the conventional ECA. The hybrid ECA with a relatively small amount of silver fillers displayed a bulk resistivity comparable to that of a eutectic solder.

2. Experimental Section

2.1. Synthesis of Ag NBs

The Ag NBs were synthesized by chemical reduction of silver nitride (AgNO_3 , Sigma–Aldrich) in the presence of poly(methacrylic acid) (PMAA) according to our recent work.^[25] In detail, 2.1 g of AgNO_3 was dissolved into 60 mL of de-ionized (DI) water and agitated in an ultrasonic bath for 10 min. Separately, 0.4–1 g reducing agent of ascorbic acid (Alfa Aesar) and a small amount of aqueous solution of PMAA sodium salt (40%, Aldrich Chemistry) were dissolved into 200 mL of DI water and agitated in an ultrasonic bath for 10 min. The synthesis was started by adding the AgNO_3 solution into the reducing solution while they were stirred gently by a magnetic stirrer. After 10 min, solid precipitates were collected by vacuum filtering and dried in a vacuum oven at room temperatures afterwards.

2.2. Nanocomposite Preparation

The synthesized Ag NBs along with Ag flakes (Aldrich, $10\ \mu\text{m}$) at different weight fractions were added to epoxy (diglycidyl ether of bisphenol A, DERTM 322, DOW chemical company, USA). The weight fractions of the micro- and nano-fillers are listed in Table 1. To ensure a good dispersion of the NBs in the viscous epoxy, the NBs were first dispersed in isopropyl alcohol (IPA). The NB suspension was then added to the mixture of Ag flakes and epoxy, which was

Table 1. Weight fractions of silver NBs and silver flakes in the conventional and hybrid ECA samples.

	Sample	Ag NB [mg]	Ag flake [mg]	NB concentration [wt.-%]	K = Ag NB/ Ag flake	Total filler concentration [wt.-%]
Conventional ECA	1	0	200	0	0	60
	2	0	210	0	0	61
	3	0	220	0	0	62
	4	0	230	0	0	63
	5	0	240	0	0	64
	6	0	564	0	0	81
Hybrid ECA	7	7	200	2	0.03	61
	8	18	200	5	0.09	62
	9	30	200	8	0.15	63
	10	40	200	11	0.2	64
	11	17	547	2	0.03	81

slightly diluted by IPA. The mixture was agitated for 30 min using a vortex mixer followed by 1 h of sonication; then, the mixture was degassed under vacuum for 1.5 h to remove the solvent from the system. After degassing, the curing agent triethylenetetramine (TETA, DOW chemical company, USA) was added to the mixture. The weight ratio of the curing agent to epoxy was 0.13. The final mixture was filled into a mold of $7 \times 7 \times 0.5 \text{ mm}^3$ ($L \times W \times D$) made on a pre-cleaned microscope glass slide using pieces of adhesive tape. To make a smooth surface and control the sample thickness, a clean copper plate was placed on top of the mold; the extra material was squeezed out. The samples were pre-cured for 30 min at 60°C and then cured at 150°C for 2 h. After curing, the copper plate and adhesive tape were manually peeled off. The same procedure was applied to prepare conventional ECAs (epoxy and Ag flakes) except, there were no Ag NBs in the system.

2.3. Characterization Methods

A standard differential scanning calorimeter (DSC, TA Instruments, Q 2000) was used to estimate the debonding temperature between the covering layer (PMAA) and the Ag NBs. In DSC tests, a sample of about 6 mg was placed into a hermetically sealed pan and placed into the DSC cell under a nitrogen purge at $50 \text{ mL} \cdot \text{min}^{-1}$. The first heating scans were performed at a rate of $10^\circ\text{C} \cdot \text{min}^{-1}$. After the first scan, the sample was cooled down to room temperature and then re-scanned at the same heating rate. The sample weight-loss and the NBs surface coverage with PMAA were studied using thermogravimetric analysis (TGA, TA instrument, Q500-1254). A sample of about 10 mg was placed into the TGA sample pan. Dynamic scan was performed from 40 to 700°C with a heating rate of $10^\circ\text{C} \cdot \text{min}^{-1}$ under a $50 \text{ mL} \cdot \text{min}^{-1}$ nitrogen purge atmosphere. The morphologies of the NBs and cured nanocomposites were examined by scanning electron microscope (SEM, LEO FE-SEM 1530, Carl Zeiss NTS) operating at 10 kV and high resolution transmission electron microscope (HRTEM, JEOL 2010F FEG) operating at 200 kV. For the cross-sectional analysis by SEM, samples were kept in liquid

nitrogen bath for 10 min and gently broken while they were in the bath. The samples were mounted vertically on an SEM stub and SEM images were taken from the cross-section. The surface quality of the ECA nanocomposites was examined by water contact angle measurement tests along with surface roughness analysis. Water contact angle measurement tests were performed by placing six water droplets of $\approx 3 \mu\text{L}$ on different spots on the sample surface. The static water contact angles on pure epoxy as well as on conventional and hybrid ECAs were measured by analyzing the image of each water droplet using a MATLAB code. The surface roughness of the samples was measured using a Veeco optical profilometer. The bulk electrical resistivity of the samples was measured using a four-point probe setup consisting of a probe fixture (Cascade microtech Inc.) and a source meter (Keithley 2440 5A Source Meter, Keithley Instruments Inc.). The sheet resistance of the samples (R_s) was characterized by the drop in voltage when applying a constant current (10 mA). The measurements were performed for four individual samples of a particular filler composition at five different spots; the average of all the readings was reported as the final value for that concentration. The electrical resistivity (ρ) of the nanocomposites was calculated using the following equation:

$$\rho = R_s \frac{w \cdot t}{l} \quad (1)$$

where w , l , and t are the sample width, length, and thickness, respectively.

3. Results and Discussion

High-aspect-ratio Ag NBs were fabricated by a facile chemical reduction approach based on the self-assembly and room-temperature joining of the hexagonal and

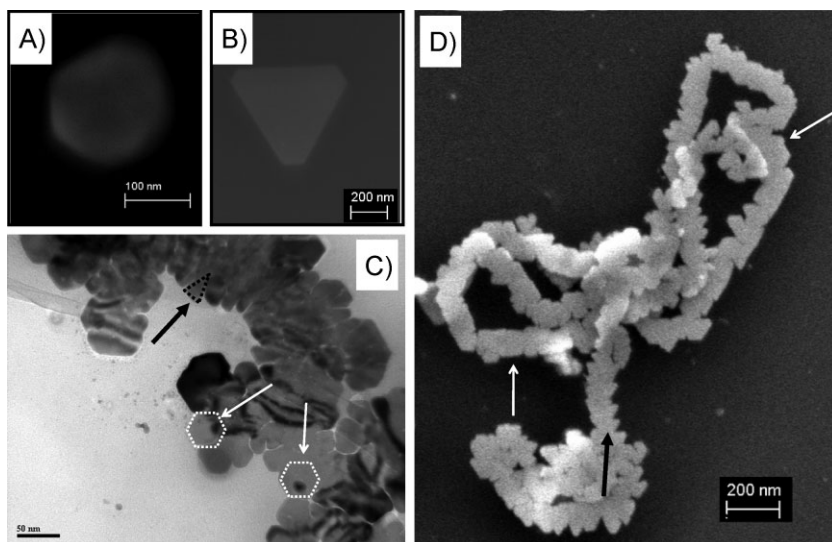


Figure 1. The SEM images of (A) a hexagonal silver NP and (B) a triangular silver NP. (C) A TEM image of the silver NB showing the self-assembly and joining of the structural blocks. (D) A SEM image of silver NBs. The white arrows point to hexagonal silver NPs and the black arrows point to triangular silver NPs.

triangular Ag NPs formed in the earlier stages of the synthesis. The synthesis mechanism is based on the reduction of silver ions by ascorbic acid to form initial silver crystals.^[25,26] The PMAA covers the (111) planes of these initial crystals, making the growth rate in the [111] direction slower than that in the [100] direction. As a result, the initial crystals grow into a hexagonal morphology, as shown in Figure 1A.^[25–29] The top and bottom planes of the hexagons are (111) planes, whereas their edges are (111) and (100) planes.^[30–32] However, throughout the synthesis process, some of the hexagons turn into triangles (see Figure 1B). The change in the morphology of hexagons is because of the difference between the growth rate of silver in [111] and [100] directions.^[31] It should be noted that, despite the hexagons, the edges of the triangular Ag NPs only consist of (100) planes.^[31,33,34]

As the top and the bottom flat faces of the hexagonal and triangular Ag NPs are covered by long-chain polymer molecules (PMAA),^[25] they join to each other from the edges and assemble linearly to form high-aspect-ratio belts.^[25,28] Figure 1C and D clearly show the way the structural blocks (as pointed by arrows) were joined to each other and assembled into belt morphology. As can be seen in Figure 1D, the NBs are wavy and their edges are not flat. This interesting morphology is formed because of the shape of the structural blocks and also due to the way they join to each other. The size analysis of NBs was performed by measuring the length and width of 1 700 randomly picked Ag NBs extracted from the SEM images. The width of the belts was in the range of 100–400 nm, whereas the majority

of the end-to-end length of the NBs, presented in Figure 2, was in the range of 1–10 μm .

Although the presence of PMAA was crucial to control the shape of the NBs and to prevent their aggregation, it should be noted that this layer, because of its insulating nature, may inhibit the electrical performance of the final nanocomposite. The amount of organic materials and their debonding temperature from the surface of conductive fillers can largely affect the final electrical properties of the ECAs.^[11,13,24] Hence, it is necessary to determine the amount of PMAA on the NBs surface and study its thermal properties. In this regard, DSC and TGA measurements were performed to determine the thermal behavior and amount of the organic layer on the NBs. Figure 3A represents the DSC curve for the Ag NBs. The first heating curve shows an endothermic peak at 150 °C, which disappeared in the second heating scan.

This peak can be attributed to the debonding of PMAA from the NBs surface.^[11] Thus, a minimum curing temperature of 150 °C is needed to detach the PMAA from the NBs surface so as to eliminate the negative effect of the covering layer on the overall conductivity of the nanocomposite. Figure 3B shows the TGA curves for both the synthesized NBs and pure PMAA. It can be seen that most of the pure PMAA (more than 95 wt.-%) was decomposed up to 200 °C. Regarding the TGA curve for NBs, there is a slight weight loss ($\approx 0.1\%$) up to 150 °C, which can be related to water evaporation. After 150 °C, an abrupt transition was observed, which finished at the temperature around 425 °C. This transition can be attributed to the thermal decomposition of the PMAA adsorbed on the surface of the NBs.^[11] The total weight loss

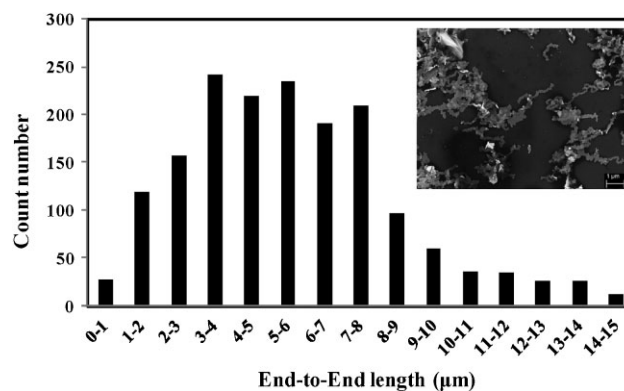


Figure 2. The end-to-end length distribution of the silver NBs. The inserted image is a typical SEM image of the silver NBs.

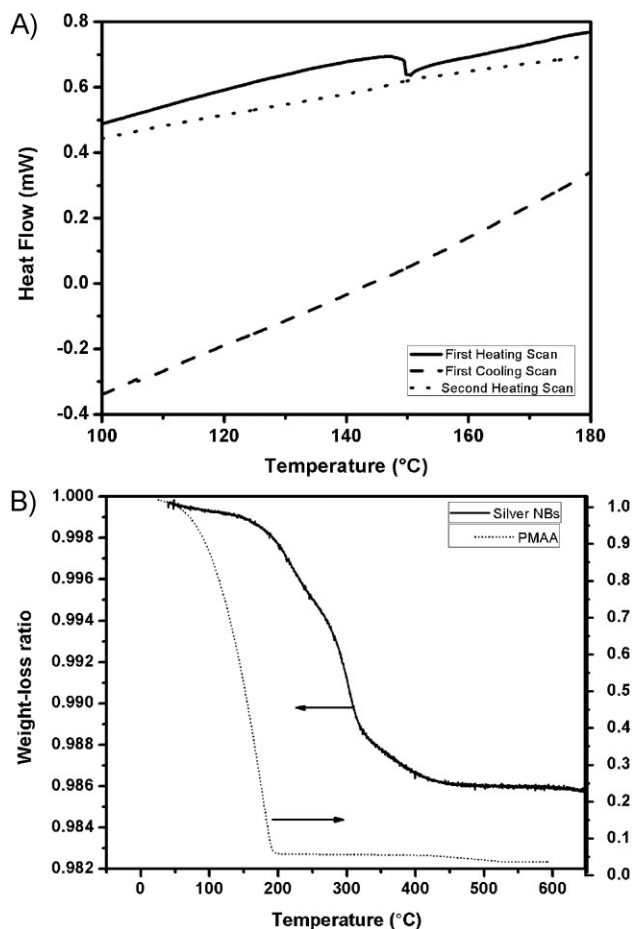


Figure 3. Thermal characterization of silver NBs. (A) DSC curves (heat flow vs. temperature) for silver NBs. (B) TGA curves (weight-loss vs. temperature) for both silver NBs and pure PMAA.

(excluding the initial weight loss) for the Ag NBs was ≈ 1.3 wt.-% up to highest applied temperature of 650 °C, which shows the amount of PMAA on the surface of Ag NBs. Having a small amount of PMAA over Ag NBs indicates that the PMAA was physically adsorbed at the surface, seeing that covalent bonding could generally lead to the attachment of a large amount of PMAA on the surface of NPs.^[35,36]

To investigate the effects of Ag NBs on the electrical performance of the hybrid ECAs at low filler contents (close to the percolation threshold concentration), Ag NBs of different amounts (0–40 mg) were added to a constant base sample which is a conventional ECA containing a constant amount (200 mg, or 60 wt.-%) of silver flakes. The weight ratios of Ag NB and Ag microflake (K) were calculated, which increased from 0 to 0.2. The addition of Ag NBs also increased the total amount or weight fraction of conductive silver fillers from 60 to 64 wt.-%. In order to have direct comparisons, conventional ECAs of same silver weight fractions as the hybrid ECAs were prepared and tested. All

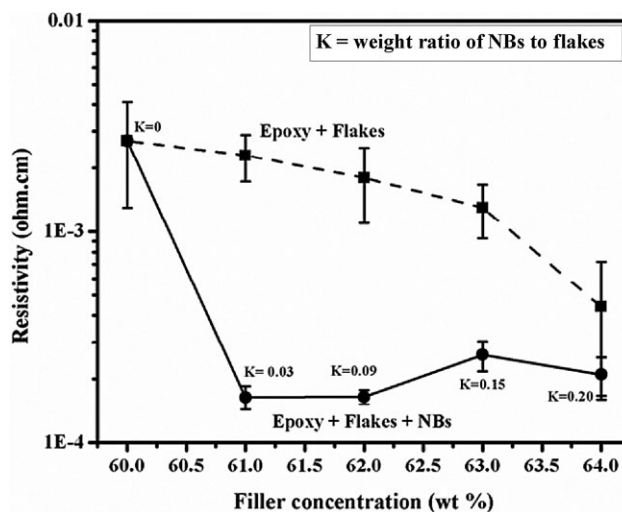


Figure 4. The bulk resistivity of the hybrid ECAs (solid line) and the conventional ECAs (dashed line) at various silver concentrations.

the samples and their composition are listed in Table 1. Figure 4 shows the changes in the bulk resistivity of the hybrid ECAs as well as that of the conventional ECAs (as the control) as the total silver weight fractions increased from 60 to 64 wt.-%; the weight ratio of Ag NBs to Ag flakes (K) are labeled beside each hybrid ECA samples. It can be seen that adding a small amount of the Ag NBs ($K = 0.03$ – 0.09) to the conventional ECAs ($K = 0$) dramatically reduced the bulk resistivity of the conventional ECAs. The minimum bulk resistivity of the hybrid ECAs with $K = 0.03$ was approximately 7% of the resistivity of the conventional ECAs with the same filler content (61 wt.-% of silver), resulting in an enhancement of conductivity by 1 300%. When more NBs were added to the system ($K = 0.15$ and 0.20), the bulk resistivity of the hybrid ECAs started to increase but only slightly. By contrast, bulk resistivity of the control conventional ECAs decreased slowly with the addition of more silver microflakes. At the weight fraction of 64%, the resistivities for the conventional and hybrid ECAs are close. These results show that adding more Ag NBs or increasing the K value did not improve ECAs further. Perhaps a large amount of nanoscale fillers caused a significant increase in the number of contact points or contact resistance among the fillers which may cancel out the positive effect of Ag NBs on adding more electrical conductive paths in the network.^[10]

It is worthwhile mentioning that during electrical resistivity measurements, it was noticed that there were some non-conductive spots on the surface of the conventional ECAs because the ECA surface was not homogeneous and the non-conductive spots contain only epoxy. By contrast, the measurements for the hybrid ECAs were quite similar all over the surface. This observation is

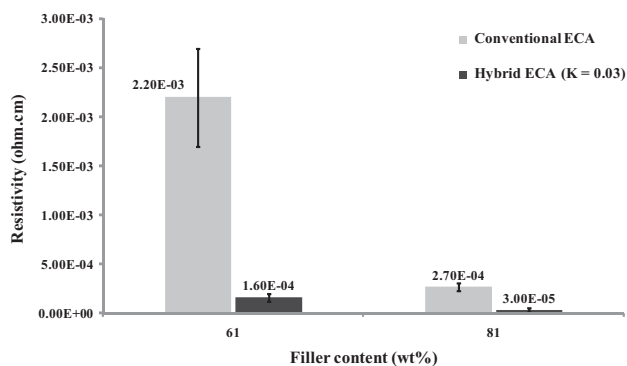


Figure 5. The comparison between the electrical resistivity of conventional and hybrid ECAs at different filler concentrations of 61 and 81 wt.-%.

reflected by smaller error bars of the data points for the hybrid ECAs in Figure 4. It seems that the incorporation of the NBs into the conventional ECAs made the surface of nanocomposites more electrically homogeneous. Furthermore, both the conventional and hybrid ECAs were observed to bond well to the glass substrate surfaces; the addition of NBs in the system has no significant effect on the adhesive bonding strength.

To further evaluate the effectiveness of the hybrid filler system in the fabricated ECA composites, the weight fraction of silver in both the conventional and hybrid ECA composites was increased from the 61 to 81 wt.-%. The bulk resistivity of the epoxy filled with 81 wt.-% of silver flakes was $2.7 \times 10^{-4} \Omega \cdot \text{cm}$, which is close to the bulk resistivity of the hybrid ECAs filled with 61 wt.-% of silver (NBs + silver flakes) ($1.6 \times 10^{-4} \Omega \cdot \text{cm}$), as shown in Figure 5. These data clearly demonstrate that using small amounts of silver NBs is more effective in reducing the electrical resistivity than adding more Ag flakes to the system. We also added 2 wt.-% ($K = 0.03$) Ag NBs to the conventional ECAs filled with 80 wt.-% silver flakes (total silver content of 81 wt.-%), which showed almost 800% better electrical conductivity (the reciprocal of the measured resistivity) in comparison to the conventional ECA filled with the same amount of silver flakes (81 wt.-%). This suggests that the effect of the NBs on the electrical conductivity enhancement of the ECAs at 61 wt.-% filler content (close to the percolation threshold) is more pronounced than that at 81 wt.-% filler content, which is beyond the percolation threshold. It is also important to note

that the bulk resistivity of the epoxy filled with 81 wt.-% of Ag NBs and Ag flakes ($K = 0.03$) was measured to be $3 \times 10^{-5} \Omega \cdot \text{cm}$. This value is comparable to that of a typical eutectic solder,^[37] demonstrating the great potential of this hybrid ECA as an alternative electrical interconnect material.

To obtain some insights into the observed electrical conductivity improvement of the hybrid filler system, the total number of filler particles in a hybrid ECA is compared with that in the conventional ECA. Considering the NBs as a rectangular cubic with dimension of $5 \mu\text{m} \times 200 \text{nm} \times 20 \text{nm}$ (length \times width \times thickness), and the flakes as a circular disc with radius of $5 \mu\text{m}$ and thickness of 500nm , the number of Ag NBs and silver flakes per gram is about 5×10^{12} and 6×10^8 , respectively. Thus, it can be stated that by adding similar amounts of NBs and silver flakes, number of NBs in the composite is almost four orders of magnitude larger than that of silver flakes. Because of the smaller size of the NBs, they can readily fill in the interstitial space among the micro flakes to have a better filler distribution at small (submicron) length scales.

The overall resistance of an electrical network comes from the bulk resistance of fillers (R_b) and the contact resistance between neighboring fillers as illustrated in Figure 6A1. The filler–filler contact resistance itself is composed of two distinct parameters: constriction resistance (R_c) and tunneling resistance (R_t). The constriction resistance comes from the spots where there is direct contact between the conductive fillers; it increases with the

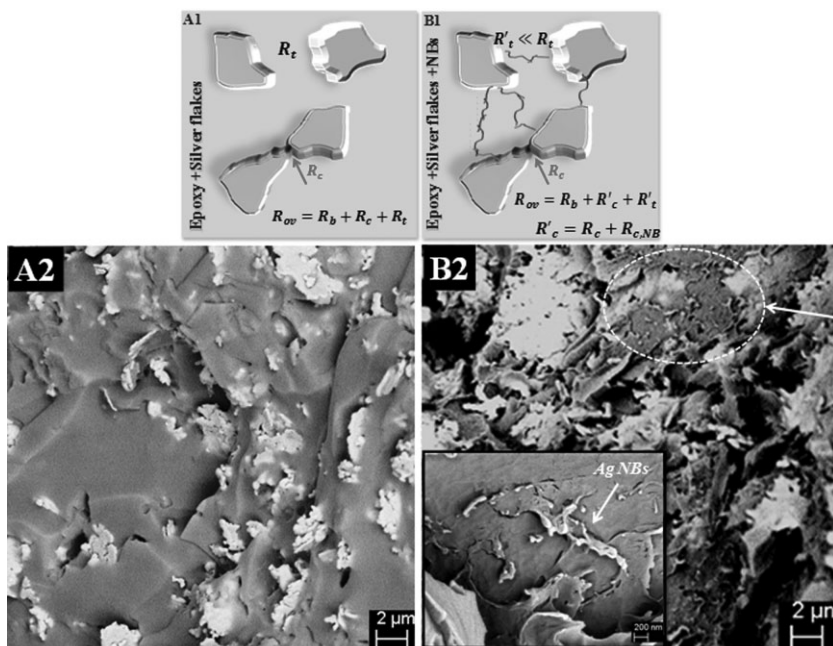


Figure 6. The schematic of the electrical network of (A1) a conventional ECA and (B1) a hybrid ECA. SEM images of the cross-sections of (A2) the conventional ECA and (B2) the hybrid ECA filled with the same amount of silver fillers (61 wt.-%). The inserted image is a high magnification SEM image of Ag NBs.

number of contact points and the sharpness of the contact. The tunneling resistance comes from the spots where there is no direct connection between conductive fillers and, therefore, electrons need to overcome barrier energy to transfer through those spots. In other words, tunneling resistance is a summation of those resistivities induced by any insulating material that inhibits the free flow of the electrons throughout the electrical network.^[10] In the ECA systems, as schematically shown in Figure 6A1 and B1, the NBs can bridge the separated Ag flakes, helping the development of more electrical paths in the hybrid ECA and as a result, having lower tunneling resistance in the case of hybrid ECA. On the other hand, a large amount of NBs may increase the number of contact points and subsequently increase the constriction resistance among the fillers, which might be detrimental to the quality of filler network. This is evidenced by the fact that increased ratio of NBs to microflakes or the *K* values in Figure 4 did not improve the conductivity. Thus, the addition of an excessive amount of NBs should be avoided.

SEM analysis was performed to verify the possible bridging effect of the NBs when adding a small amount. Figures 6A2 and B2 show the typical SEM images of the cross-sections of both the conventional and hybrid ECAs with the same (i.e., 61 wt.-%) filler concentration, respectively. As can be observed in Figure 6A2, many silver flakes in the conventional ECA are separated by epoxy; thus, the electrical network has not been completely established. By contrast, Figure 6B2 shows that in the case of the hybrid ECA, NBs bridged those separate silver flakes and made them connected (as pointed by the white arrow). It also shows that the NBs are fairly distributed throughout the epoxy; no noticeable aggregation can be observed. This observation evidenced the effectiveness of the dispersion method employed in the preparation of the hybrid filler system, which led to homogenous dispersion of the NBs throughout the nanocomposite. The inserted image of Figure 6B2 is a higher magnification SEM image of Ag NBs in the nanocomposite. It can be seen that

the structure of the NBs was preserved during the nanocomposite preparation.

The surface properties of the hybrid ECAs might be another reason for the electrical conductivity improvement of the ECAs. They were investigated by performing water contact angle tests and roughness measurements. As can be observed in Figure 7A1 and B1, adding 2 wt.-% Ag NBs to the conventional ECAs with 60 wt.-% Ag flakes (total silver

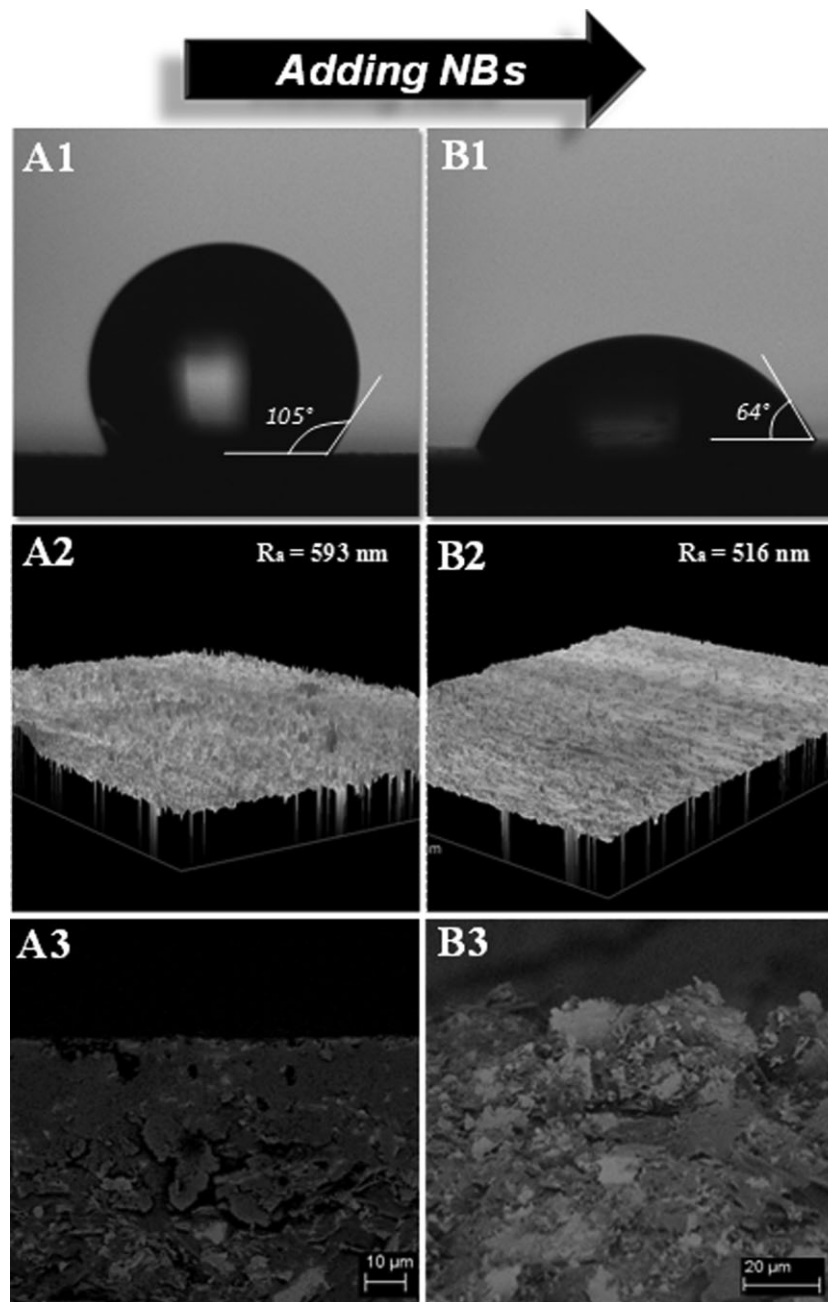


Figure 7. The water contact angles for (A1) a conventional ECA—sample 2 and (B1) a hybrid ECA—sample 7. Surface topography maps for (A2) the conventional ECA and (B2) the hybrid ECA. SEM images of the cross-sections of ECA showing the near surface composition for (A3) the conventional ECA and (B3) the hybrid ECA at a 90° view angle.

content of 61 wt.-%) decreased the water contact angle from $105^\circ \pm 5.2^\circ$ for the conventional ECA to $64^\circ \pm 7^\circ$ for the hybrid ECA. The water contact angle measurements were also performed for other hybrid samples (with 62–64 wt.-% of silver), whereas pretty much similar results (ranging from 65° to 77°) were obtained. Given that the water contact angle can be significantly affected by the topographical structure of the surface (i.e., roughness), the average surface roughness (R_a) of the conventional and hybrid ECAs were measured by Veeco optical profilometer. The typical surface profiles of both samples (having R_a of 593 ± 61 nm and 516 ± 130 nm, respectively) are presented in Figure 7A2 and B2. The surface profile of the both sample are almost similar demonstrating that the effect of surface roughness on the measured water contact angles is negligible.

The water contact angle on pure epoxy was measured to be $80^\circ \pm 5^\circ$. The water contact angle on the Ag flakes cannot be determined because of their discrete nature. In the literature, pure Ag has been reported to have a low contact angle close to 0° ,^[38] whereas Ag covered with the common surfactant stearic acid has a water contact angle about 160° .^[39] Recalling the effective contact angle of the conventional ECA as $105^\circ \pm 5.2^\circ$, it is obvious that the surface of the conventional ECA consisted of both epoxy and silver flake. However, the addition of silver NBs with the low water contact angle of 0° – 49° ^[38,40] (depending on whether the PMAA was fully or partially decomposed from the NBs surface) to the conventional ECA led to a significant decrease in the water contact angle for the hybrid ECA (i.e., from $105^\circ \pm 5.2^\circ$ for the conventional ECA to $64^\circ \pm 7^\circ$ for the hybrid ECA). Considering the small amount of silver NBs added, it can be stated that NBs have significantly enriched the surface composition, leading to improved electrical conductivity of hybrid ECAs.

SEM morphological analyses were further performed on the cross-sections of the conventional ECA as well as that of the hybrid ECA (61 wt.-% silver) to evaluate filler distribution as shown in Figure 7A3 and B3, respectively. To avoid possible distortion of filler distribution during the preparation of cross-sections, the ECA samples were frozen in liquid nitrogen and gently broken into two parts while in the liquid nitrogen bath. It can be observed in Figure 7A3 that the surface of the conventional ECA was mainly covered by epoxy, whereas the silver flakes were partially depleted from the surface. By contrast, in the case of the hybrid ECA (see Figure 7B3), the silver fillers is the dominant component occupying the near surface matrix of the composite. Although further surface analyses are needed to fully quantify the surface filler compositions. These SEM and the water contact angle analyses suggested that the introduction of the silver NBs to the system may have enhanced the fraction of conductive fillers at the surface, even though the total amount of silver fillers is still similar to that of the conventional ECA. This enrichment of silver fillers in

the hybrid ECA could contribute to the better electrical conductivity of the hybrid ECA in comparison to that of the conventional ones.

4. Conclusion

High-aspect-ratio Ag NBs were synthesized and utilized to develop a nano- and micro-hybrid filler system for the epoxy-based conductive adhesive composites. The synthesis of the Ag NBs is based on a chemical reduction of silver nitride in the presence of PMAA. It involves an innovative process of the self-assembling and room-temperature joining of hexagonal and triangular structural blocks formed at the initial stages of the synthesis to fabricate high-aspect-ratio NBs. The DSC and TGA analyses showed that only a small amount of PMAA physically adsorbed on the NBs surface, whereas the attached polymer can be detached from the surface at 150°C . The high-aspect-ratio NBs were successfully incorporated to the system of conventional ECAs consisting of silver flakes and epoxy to make hybrid ECAs of superior electrical properties. It was found that the hybrid ECAs always displayed lower electrical resistivity than the conventional ECAs. Particularly, the introduction of a small amount of the Ag NBs (weight ratio of the NBs to flakes $K=0.03$) into a conventional ECA with 60 wt.-% micron-sized silver flakes resulted in an electrical conductivity enhancement by 1300% in comparison to that of the conventional ECAs with the same total silver weight fraction (61 wt.-%). The conductivity enhancement comes from the bridging of Ag NBs among the silver microflakes. The addition of a larger amount of Ag NBs did not improve the conductivity further because it increased the number of contact points and subsequently the contact resistance among the fillers, which might cancel out the positive effect of bridging on the quality of filler network. Other than the bridging effect of Ag NBs in the hybrid ECAs, the SEM and the water contact angle analyses suggested that the introduction of the Ag NBs to the system may have enhanced the fraction of conductive fillers at the surface, even though the total amount of silver fillers is still similar to that of the conventional ECA. This might be another reason for the electrical conductivity improvement of the ECAs. Moreover, it was found that adding a 2 wt.-% ($K=0.03$) of the NBs into a ECA with 80 wt.-% Ag flakes reduced the bulk resistivity to $3 \times 10^{-5} \Omega \cdot \text{cm}$, which is comparable to that of a typical eutectic solder, showing a great potential of the fabricated hybrid ECA as an alternative electrical interconnect material.

Acknowledgements: This work was supported by the research funds from the Natural Sciences and Engineering Research Council of Canada (NSERC).

Received: July 19, 2013; Revised: August 26, 2013; Published online: November 24, 2013; DOI: 10.1002/mame.201300295

Keywords: electrical conductive adhesive; electrical properties; high-aspect-ratio nanofillers; hybrid composite; silver nanobelts

- [1] V. H. Luan, H. N. Tien, T. V. Cuong, B. Kong, J. S. Chung, E. J. Kim, S. H. Hur, *J. Mater. Chem.* **2012**, *22*, 8649.
- [2] T. Akter, W. S. Kim, *ACS Appl. Mater. Interface* **2012**, *4*, 1855.
- [3] R. Zhang, J. C. Agar, C. P. Wong, *12th Electron. Packag. Tech. Conf.*, Singapore **2010**.
- [4] S. Bohm, E. Stammen, G. Hemken, M. Wanger, *Microjoining and Nanojoining*, Vol. 1, Y. Ed., CRC Press, Boca Raton, Florida, USA **2008**, Ch. 17.
- [5] Oh, Y. Zhou, K. Chun, E. Lee, Y. Kim, S. Baik, *J. Mater. Chem.* **2010**, *20*, 3579.
- [6] C. Chen, L. Wang, R. Li, G. Jiang, H. Yu, T. Chen, *J. Mater. Sci.* **2007**, *42*, 3172.
- [7] K. Chun, Y. Oh, J. Rho, J. Ahn, Y. Kim, H. R. Choi, S. Baik, *Nature* **2010**, *5*, 853.
- [8] Y. Tao, Y. Xia, H. Wang, F. Gong, H. Wu, G. Tao, *IEEE Trans. Adv. Pack.* **2009**, *32*, 589.
- [9] W. Jeong, H. Nishikaw, D. Itou, T. Takemoto, *Mater. Trans.* **2005**, *46*, 2276.
- [10] B. M. Amoli, S. Gumfekar, A. Hu, Y. N. Zhou, B. Zhao, *J. Mater. Chem.* **2012**, *22*, 20048.
- [11] J. Jiang, K. Moon, Y. Li, C. P. Wong, *Chem. Mater.* **2006**, *18*, 2969.
- [12] Y. Long, J. Wu, H. Wang, X. Zhang, N. Zhao, J. Xu, *J. Mater. Chem.* **2011**, *21*, 4875.
- [13] R. Zhang, K. Moon, W. Lin, J. C. Agar, C. P. Wong, *Compos. Sci. Technol.* **2011**, *25*, 528.
- [14] L. Ye, Z. Lai, J. Liu, A. Thölen, *IEEE Trans. Electron. Pack.* **1999**, *22*, 299.
- [15] H. P. Wu, J. F. Liu, X. J. Wu, M. Y. Ge, Y. W. Wang, G. Q. Zhang, J. Z. Jiang, *Int. J. Adhes. Adhes.* **2006**, *26*, 617.
- [16] Y. Oh, D. Suh, Y. Kim, E. Lee, J. S. Mok, J. Choi, S. Baik, *Nanotechnology* **2008**, *19*, 1.
- [17] R. Ma, S. Kwon, Q. Zheng, H. Y. Kwon, J. I. Kim, H. R. Choi, S. Baik, *Adv. Mater.* **2012**, *24*, 3344.
- [18] Y. Tao, Y. P. Xia, G. Q. Zhang, H. P. Wu, G. L. Tao, *Proc. SPIE* **2009**, *7493*, 1.
- [19] F. Marcq, P. Demont, P. Monfraix, A. Peigney, Ch. Laurent, T. Falat, F. Courtade, T. Jamin, *Microelectron. Reliab.* **2011**, *51*, 1230.
- [20] J. Feng, X. Ma, H. Mao, B. Liu, X. Zhao, *J. Mater. Res.* **2011**, *26*, 1.
- [21] D. Chen, X. Qiao, X. Qiu, F. Tan, J. Chen, R. Jiang, *J. Mater. Sci. Mater. Electron.* **2010**, *21*, 486.
- [22] Y. H. Yu, C. C. M. Ma, S. M. Yuen, C. C. Teng, Y. L. Huang, I. Wang, M. H. Wei, *Macromol. Mater. Eng.* **2010**, *295*, 1017.
- [23] H. P. Wu, X. J. Wu, M. Y. Ge, G. Q. Zhang, Y. W. Wang, J. Z. Jiang, *Compos. Sci. Technol.* **2007**, *67*, 1116.
- [24] Z. X. Zhang, X. Y. Chen, F. Xiao, *J. Adhes. Sci. Technol.* **2011**, *25*, 1465.
- [25] E. Marzbanrad, A. Hu, B. Zhao, Y. Zhou, *J. Phys. Chem. C.* **2013**, *117*, 16665.
- [26] W. Songping, M. Shuyuan, *Mater. Chem. Phys.* **2005**, *89*, 423.
- [27] A. R. Tao, S. Habas, P. Yang, *Small* **2008**, *4*, 310.
- [28] D. Spadaro, E. Barletta, F. Barreca, G. Curro, F. Neri, *Appl. Surf. Sci.* **2010**, *256*, 3812.
- [29] D. Zhang, L. Qi, J. Ma, H. Cheng, *J. Chem. Mater.* **2001**, *13*, 2753.
- [30] J. L. Elechiguerra, J. Reyes-Gasga, M. J. Yacaman, *J. Mater. Chem.* **2006**, *16*, 3906.
- [31] D. Aherne, D. M. Ledwith, M. Gara, J. M. Kelly, *Adv. Funct. Mater.* **2008**, *18*, 2005.
- [32] X. Lu, M. Rycenga, S. E. Skrabalak, B. Wiley, Y. Xia, *Annu. Rev. Phys. Chem.* **2009**, *60*, 167.
- [33] M. Maillard, S. Giorgio, M. P. Pileni, *Adv. Mater.* **2002**, *14*, 1084.
- [34] V. Germain, J. Li, D. Inger, Z. L. Wang, M. P. Pileni, *J. Phys. Chem. B.* **2003**, *107*, 8717.
- [35] D. E. Cliffl, F. P. Zamborini, S. M. Gross, R. W. Murray, *Langmuir* **2000**, *16*, 9699.
- [36] S. Chen, K. Kimura, *Langmuir* **1999**, *15*, 1075.
- [37] C. Yang, C. P. Wong, M. F. Yuen, *J. Mater. Chem. C* **2013**, DOI: 10.1039/c3tc00572k.
- [38] F. E. Bartell, P. Cardwe, *JACS* **1942**, *64*, 494.
- [39] A. Safaee, D. K. Sarkar, M. Farzaneh, *Appl. Surf. Sci.* **2008**, *254*, 2493.
- [40] R. Heeb, R. M. Bielecki, S. Lee, N. D. Spencer, *Macromolecules* **2009**, *42*, 9124.